Applied Catalysis B: Environmental 140–141 (2013) 169–178

Contents lists available at SciVerse ScienceDirect

Applied Catalysis B: Environmental

journal homepage: www.elsevier.com/locate/apcatb

# Photocatalysis on yeast cells: Toward targets and mechanisms

Sana Thabet[a,b], Michele Weiss-Gayet[c], Frederic Dappozze[a], Pascale Cotton[b,1], Chantal Guillard[a,*,1]

[a] Université de Lyon, Université Lyon 1, CNRS, UMR 5256, IRCELYON, Institut de Recherches sur la Catalyse et l'Environnement de Lyon, 2 avenue Albert Einstein, F-69626 Villeurbanne, France
[b] Université de Lyon, Université Lyon1, CNRS-UCB-INSA-BCS, UMR 5240, Génétique Moléculaire des Levures, Microbiologie,Adaptation et Pathogénie, Domaine scientifique de la Doua, 10 rue Raphaël Dubois, bâtiment Lwoff, F-69626 Villeurbanne, France
[c] Université de Lyon, Université Lyon 1, UMR 5534, Centre de Génétique et de Physiologie Moléculaire et Cellulaire, 16 rue Raphaël Dubois, bâtiment Gregor Mendel, F-69626 Villeurbanne, France

ARTICLE INFO

*Article history:*
Received 11 January 2013
Received in revised form 10 March 2013
Accepted 21 March 2013
Available online 30 March 2013

*Keywords:*
Photocatalysis
Yeast
Viability
Cytometry
Byproducts

ABSTRACT

We have investigated the antimicrobial effects of photocatalysis on yeast (*Saccharomyces cerevisiae*), an essential eukaryotic unicellular model of living cells. As compared to UV-A irradiation, photocatalytic inactivation kinetics revealed a faster microbial cell cultivability inactivation. Optimal experimental conditions required a semiconductor concentration of 0.1 g/l with 3.8 mW/cm$^2$ UV-A radiance intensity. Cell viability was monitored by plasma membrane permeability and loss of enzymatic activity using double fluorescent dye staining and flow cytometry. Plasma membrane permeability and enzymatic activity were almost simultaneously targeted. Esterase enzymatic activity decreased progressively, suggesting that the intracellular protein pool was sequentially damaged by the treatment. In yeast cells, the presence of a thick cell wall did not prevent the plasma membrane from being a prime photocatalytic target. Monitoring of chemical byproducts confirmed the loss of membrane integrity. A massive loss of potassium, major cation in yeast, that was released first and in large amounts, remained constant beyond 5 h of treatment and was correlated to the number of damaged membrane-cells. On the contrary, ammonium ions concentration gradually increased, suggesting their generation through the photocatalytic process, probably via amino acid and protein degradation. Oxamic and oxalic acid that could also arise from damages to amino acids were detected. Amino acid analysis revealed a main component, increasing over time, corresponding to glycine. Glycine could be produced via the transformation of other amino acids, released from cell wall, membrane and intracellular proteins.



## 1. Introduction

As an alternative to conventional chemical disinfection technologies, advanced oxidation processes receive currently considerable attention. Among them, photocatalysis has emerged as a widely recognized powerful antimicrobial agent by providing an alternative to biocides [1–6]. Nowadays, titanium dioxide ($TiO_2$) is the most widely used photocatalyst because of its relative high photocatalytic activity, its availability and relative low cost.

$TiO_2$ photocatalysis reaction has been well described [7,8]. Briefly, absorption of UV radiations of energy equal or greater than the photocatalyst band gap energy generates $e^-/h^+$ pairs. In aqueous environments, these photogenerated species react on the surface of $TiO_2$ particles and induce highly reactive oxygen species (ROS): $O_2^{\bullet -}$, $^\bullet OH$ and $H_2O_2$. Hydroxyl radical is considered as the main oxidant, responsible for inactivating microorganisms [9,10].

The antimicrobial efficiency of photocatalysis was described for the first time by Matsunaga in 1985 [11] using $TiO_2$/Pt as a catalyst. Numerous subsequent studies were then dedicated to describe the antimicrobial effect of $TiO_2$ photocatalysis. Because of their omnipresence in the environment and their strong impact on human health associated with recurrent antibiotic resistance spreading, bacteria have been the more extensively studied microorganisms. Various Gram negative and Gram positive bacteria mainly implicated in commensalism or pathogenic relationship with humans and animals have shown to be inactivated by photocatalysis [2,12]. However, the great majority of studies have been performed with the Gram negative model bacteria *Escherichia coli* [4,6,9,13–19]. More than 35 different *E. coli* strains have been treated and inactivated by $TiO_2$ provided as suspension or coated thin films or filters [2]. Despite a high number of publications, the nature of the processes leading to cell death is still debated. Depletion of coenzyme A and subsequent inhibition of respiration was first suggested as a mechanism of

* Corresponding author at: 2 avenue Albert Einstein, F-69626 Villeurbanne, France. Tel.: +33 472445316; fax: +33 472445399.
*E-mail address:* chantal.guillard@ircelyon.univ-lyon1.fr (C. Guillard).
[1] C. Guillard and P. Cotton contributed equally to the design of this work.

0926-3373/$ – see front matter © 2013 Elsevier B.V. All rights reserved.
http://dx.doi.org/10.1016/j.apcatb.2013.03.037

killing bacteria [11,20]. Several authors suggest a drastic oxidative stress, generated by direct contact of activated $TiO_2$ on the cell surface [15,21]. Exposure to the photocatalytic treatment compromises cellular integrity, mainly by creating deleterious damages to cellular envelopes (outer and plasma membrane), thus generating leakage of cellular components and loss of cell viability [3,15,16,19,22].

However, understanding how photocatalytic processes leading to death differ among distinct groups of microorganisms, is a main concern. Indeed, mostly originating from soil and disseminated by air and water, fungi are microorganisms that are omnipresent in the environment and make an essential contribution to the biosphere. However, they can be extremely destructive, feeding on almost any kind of material and causing food spoilage and many plant diseases. Fungi are also implicated in life threatening infections in humans and animals as well as severe asthma and allergic diseases [23,24]. Fungi belong to a kingdom of eukaryotic organisms lacking chlorophyll and feeding on organic matter. The biology of eukaryotic cells is significantly different from that of bacteria in fundamental ways. Contrary to prokaryotic organisms, the eukaryotic fungal cell possesses a membrane-bound nucleus protecting DNA, and a compartmented subcellular organization constituted by organelles (Fig. 1). Their envelope is constituted, from the inside to outside, by a plasma membrane (lipid bilayer interspersed with globular proteins) and differs from bacteria by a thick prominent cell wall comprising 15–25% of the dry mass of the cell. The main structural constituents of yeast walls are polysaccharides (80–90%) but other components include mannoproteins, lipids and inorganic phosphate [25]. Yeast cytoplasm delimited by the plasma membrane is an aqueous acidic colloidal fluid containing soluble macromolecules like proteins or sugars. The rules for transmission of genetic material and some basic aspects of metabolism and regulation also differ.

Our present study was conducted on the most intensively studied eukaryotic unicellular fungus, the yeast *S. cerevisiae*, an ovoid cell (5–10 μm long) which reproduces by budding. Choosing this model offers several advantages. First, its cellular structure and functional organization has many similarities with mammalian cells [26]. Therefore, *S. cerevisiae* is a popular and successful model system for understanding eukaryotic cell behavior at both cellular and molecular level. Secondly, *S. cerevisiae* presents the advantages of unicellular organisms as it has a short generation time and can be easily cultured. Thirdly, *S. cerevisiae* appears to be a good model for studying inactivation of yeast pathogens that cause disease in humans like *Candida albicans*, but also of fungal environmental contaminants. Since the first report from Matsunaga et al., [11] that described the sterilization of *S. cerevisiae* fungal cells by $TiO_2$/Pt, studies conducted on eukaryotic microorganisms like fungi are scarce and disparate. Most of them describe fungal cells inactivation with the aim to characterize the antimicrobial efficiency of $TiO_2$-coated surfaces [27,28] or to document photocatalytic inactivation properties in the framework of plant protection and phytopathogens [29–31]. Consequently, it is of great interest to investigate in details the effects of photocatalysis on eukaryotic fungal cells.

The aim of this work was to study the effects of photocatalysis on yeast cells. Loss of cultivability and viability were correlated to damages to the plasma membrane followed by a loss of intracellular enzymatic activity. Investigations by fluorescence microscopy associated to chemical analyzes allowed to correlate the loss of cellular integrity to the release and generation of byproducts in the environment.

## 2. Experimental

### 2.1. Photocatalyst

Commercial titanium dioxide P-25 powder (Degussa AG, Germany) was used for all experiments. It is constituted by 80% anatase and 20% rutile, with an average size of 30 nm and a density of 3.8 g/cm$^2$.

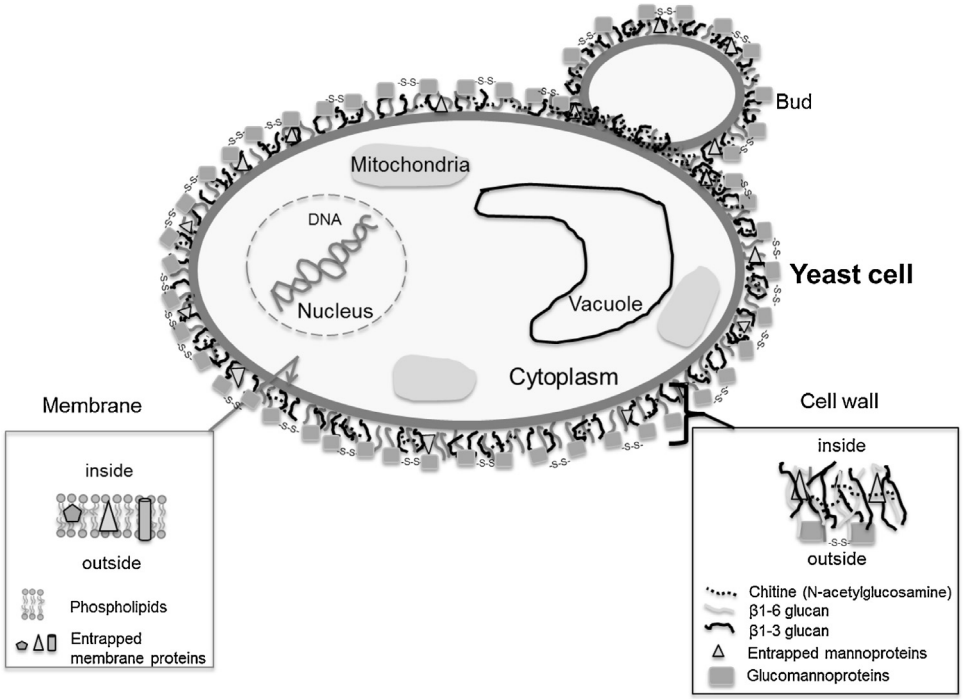


**Fig. 1.** Schematic yeast cell structure.

### 2.2. Yeast strains and growth media

The laboratory strain *S. cerevisiae* (BY4742) was used for all yeast inactivation experiments. The strain was maintained on YPD medium (1% yeast extract, 1% peptone, 2% glucose, 2% agar for plates).

### 2.3. Reactor and light source

All photocatalytic experiments were performed in a 90 ml cylindrical Pyrex reactor with an optical window diameter of 3.6 cm and containing 20 ml of yeast cell suspension. Experiments were carried out with an HPK 125 W mercury lamp cooled with a water circulation system. The light spectrum of the lamp was cut off below 340 nm using 0.52 or 7830 filter, keeping only UV-A wavelength (365 nm) and visible light. Total UV radiance intensity received by yeast suspensions was measured by a digital radiometer (VLX-3W, UVItec) equipped with 365 nm ± 5% detector and was of 3.8 mW/cm$^2$ for all experiments, except for UV intensity effect analyzes.

### 2.4. Sample preparation and photocatalytic experiments

Yeast cells were grown in liquid YPD overnight under aerobic conditions with constant shaking at 28 °C. Yeast culture growth was checked by measuring optical density at 600 nm using a spectrophotometer. For all experiments, cell samples were collected at the beginning of the exponential growth phase ($OD_{600}$ = 1,) washed twice and suspended in the photoreactor in 20 ml of sterile ultrapure (UP) water (Simplicity$^{TM}$, Millipore), with or without $TiO_2$ at a concentration of $10^7$ cells/ml. During treatment, continuous mixing was assured by magnetic stirring and all reactions were conducted at room temperature using indoor air as oxidant. For all experiments, cells were initially placed in the dark during 30 min before exposure to UV-A. UP water, $TiO_2$ and photochemistry controls were performed by incubating cells in UP water, in UP water supplemented with non-activated $TiO_2$ (in the dark), and in UP water under UV-A exposure, respectively.

To evaluate the impact of the reaction medium, complete synthetic medium (0.67% yeast nitrogen base (Difco$^{TM}$,BD), 2% glucose and amino acids (arginine: 2 mg/ml, histidine: 2 mg/ml, isoleucine: 0.6 mg/ml, leucine: 0.6 mg/ml, lysine: 0.4 mg/ml, methionine: 0.2 mg/ml, phenylalanine: 0.6 mg/ml, threonine: 0.5 mg/ml, tryptophan: 0.4 mg/ml, valine: 1.5 mg/ml) was used to resuspend cells for treatment, instead of UP water suspension.

### 2.5. Cultivability assays

Samples were collected at regular intervals during yeast inactivation reaction. Serial dilutions were immediately made in liquid YPD medium and spread onto YPD agar plates. After 2 days of incubation at 28 °C, colony forming units (CFU) detected on appropriate dilution plates were counted in order to determine the concentration of surviving cells. Three replica plates were used for each dilution of three samplings. Whole experiments were performed in three replicates.

### 2.6. Optical epifluorescence microscopy

Microscopy observations were performed using Axioscop 2 plus Zeiss optical microscope equipped with AxioCam MRm camera. Data were collected using AXioVision software.

Cell viability was investigated using PI (Propidium iodide, Invitrogen, ex/em 490/635 nm) and CFDA-AM dye (Carboxyfluorescein diacetate- acetoxymethyl, ROCH, ex/em 492/517 nm). PI enters only cells with damaged cytoplasmic membranes, whereas CFDA-AM enters all cells and is non-fluorescent until it is cut-off by active cytoplasmic esterases. CFDA-AM reflects cell metabolic activity. Treated cell samples (100 μl) were diluted in PBS to $10^6$ cells/ml. After addition of dyes (1 μg/ml IP and 5 μg/ml CFDA-AM), the mix was incubated for 20 min at 37 °C.

Cell shape was analyzed using Calcofluor white (fluka, SIGMA-ALDRICH, ex/em 355/433 nm) dye. Calcofluor white dye was added to treated cell samples that were incubated 30 min at 37 °C, washed with PBS and observed by microscopy.

### 2.7. Flow cytometry

Flow cytometry was carried out using FACS CantoII instrument (BD Biosciences) fitted with three lasers: blue (488 nm, aircooled, 20 mW solid state), red (633 nm, 17 mW HeNe) and violet (405 nm, 30 mW solid state). Diffracted light (related to cell surface: Forward scatter FSC) and reflected light (related to granularity: Side scatter SSC) of blue laser, as well as CFDA-AM and PI, were collected. Data from 10,000 cells were collected using FACSDIVA software (6.1.2 version, BD Biosciences).

### 2.8. Determination of amino acids

Detection of amino acids in the filtrates of treated cells suspension were performed using OPA and FMOC derivatization protocol followed by a HPLC analysis (Agilent 1290 Infinity). During the time course of the photocatalytic reaction, samples were removed at time intervals, filtered through 0.45 μm PVDF Millipore disc to remove $TiO_2$ powder and yeast cells. HPLC analyzes were performed using an Agilent Zorbax Eclipse AAA Rapid Resolution column (4.6 × 15 mm, 3.5 μm). Derivatization was executed on the autosampler with an injector program. Eluents were a solution of disodium phosphate and sodium tetraborate (pH 8.2) and a mix of acetonitrile, methanol and water (45/45/10). Flow rate was 2 ml/min and data were collected using Chem32 software.

### 2.9. Determination of ions and carboxylic acids

For anions ($SO_4^{2-}$, $Cl^-$ $NO_2^-$and $NO_3^-$,) and cations ($K^+$, $Na^+$ and $NH_4^+$) concentration measurement, treated cells were removed from samples by filtration through 0.45 μm PVDF Millipore disc. Ions were detected and quantified in treatment medium by ionic chromatography Metrohm using the Metrosep C4 (150 mm × 4 mm) column for cations analysis. The eluent was nitric acid (1.7 mM) and dipicolinic acid (0.7 mM) with a flow rate of 0.9 ml/min. For anions analysis, Metrosep A Supp 5 (150 mm × 4 mm) column was used. The eluent was sodium carbonate (3.2 mM) and sodium bicarbonate (1 mM) solution with a flow rate of 0.7 ml/min.

Generated carboxylic acids were analyzed in treatment medium after cell removal by filtration, by HPLC Varian ProStar 230 analysis, using a COREGEL 87H 3 (300 mm × 7.8 mm) and a Varian Prostar 330 detector (detection at 210 nm). Injection volume was 50 μl, mobile phase was sulfuric acid (5 mM) with a flow rate of 0.7 ml/min.

## 3. Results and discussion

### 3.1. Impact of photocatalysis on S. cerevisiae yeast cultivability

In order to treat a homogenous population of cells, yeasts were collected at early exponential growth phase. At this stage, cells were actively dividing and metabolically active. Effect of photocatalysis on *S. cerevisiae* yeast cultivability was investigated by using cells

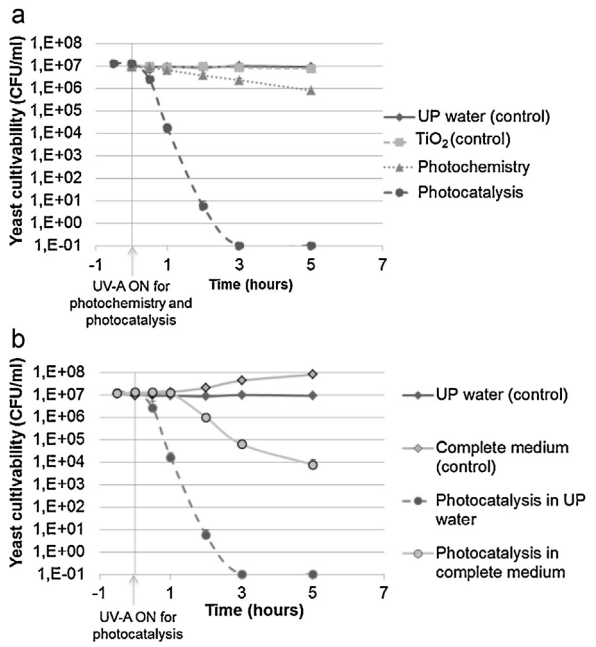


**Fig. 2.** Monitoring yeast cultivability on YPG medium. (a) Cells were suspended in UP water for exposure to UV-A photocatalysis ( ), UV-A photochemistry ( ), $TiO_2$ control ( ) and UP Water control ( ), (b) Inactivation of *Saccharomyces cerevisiae* without irradiation in UP water ( ) and complete synthetic medium ( ) and during photocatalysis in UP water ( ) or complete synthetic medium ( ). 3.8 mW/cm$^2$ UV-A and 0.1 g/l $TiO_2$.

suspended in UP water in order to avoid any interference with solubilized constituents.

Survival of control cells incubated in UP water for 5 h (Fig. 2a) was not affected. Indeed yeasts are ubiquitous fungi that develop osmoadaptation strategies that render them able to survive sudden changes in the water activity and more precisely hypoosmotic shock [32]. Cells suspended in UP water with non-activated $TiO_2$ (0.1 g/l) were slightly affected after 5-h exposure to $TiO_2$ particles. Indeed, yeast cell cultivability decreased by 30% (Fig. 2a). Previous studies have revealed an absence of toxicity for $TiO_2$ nanoparticles on *S. cerevisiae* cells [33]. $EC_{50}$ were found to be higher than 20 g/l. However, experimental conditions were drastically different from those we used. Malt extract medium containing high amounts of polysaccharides was used for toxicity testing. Exposing yeast cells to UV-A irradiation revealed more efficient to inactivate yeast cells (Fig. 2a). Cultivability decreased by 30% after one hour and by 90% after 5 h of exposure. Similar experiments, conducted on *E. coli* bacterial cells using the same total radiance intensity (3.8 mW/cm$^2$) revealed a deleterious action of UV-A on cell cultivability [19]. It is admitted that UV-A radiations provoke less deleterious effects than UV-B and UV-C on cell survival. However, oxidation reactions that mainly damage DNA molecules (mostly bases modifications and DNA strand breaks) occur in yeast cells exposed to UV-A radiations [34]. Knowing that nucleobases weakly absorb wavelengths above 320 nm, most of the damaging effect of UV-A on cellular DNA involves photosensitization reactions leading to photo oxidations within cells [35].

After one hour of exposure to photocatalytic treatment, only 0.1% of yeast cells were still cultivable (Fig. 2a). The inactivation curve of cells treated with both UV-A and $TiO_2$ was composed of two kinetic parts. During the first 30 min, the percentage of cultivable cells dropped drastically and rapidly. 20% of the cells remained cultivable after 30 min of exposure to photocatalysis, while 100% and 90% of the cells treated with non-activated $TiO_2$ and by photochemistry were still able to grow, respectively. From 1 h, cultivable targeted cells remained fewer (10,000 CFU/ml) and a longer exposure time was necessary to inactivate them. An increasing number of dead cells could form a screen and protect living cells from radiations therefore competing with living targets. Moreover, released products from inactivated cells could also interfere in the cell/particle/radiation balance and contribute to a decrease of efficiency. Comparison of inactivation kinetics during exposure to photocatalysis and control experiments ($TiO_2$, UP water, and UV-A photochemistry) revealed that photocatalysis has a decimal reduction time (90% of inactivation) of only 30 min whereas photochemistry required about 4.5 h (Fig. 2a).

Cell environment is an important parameter of the photocatalytic treatment due to direct or indirect reactions of $TiO_2$ with compounds found in microbial culture media [15,36,37]. In order to investigate its effect on yeast, we performed experiments in a conventional yeast growth medium. Complete synthetic medium contains glucose, amino acids, a series of vitamins and growth factors. After 5 h of incubation without treatment, a 10% increase of cultivable cells was observed in complete medium (Fig. 2b). Moreover, effect of photocatalysis on cultivability was clearly limited. Indeed, after 5 h of exposure, cultivable cell number decreased from $10^7$ to $10^4$ CFU/ml, while this was performed in one hour in UP water (Fig. 2b). Loss of cultivability occurred immediately after starting UV-A exposure in UP water, while it started decreasing only after 1 h in complete medium. This suggests that organic compounds contained in complete synthetic medium are in competition with cells during photocatalysis process. Indeed, degradation of organic compounds in $TiO_2$ photocatalysis has been demonstrated [7,8,36,37]. Thus, complete synthetic medium promotes cell division and growth. Therefore, multiplication of the survival yeasts could partially compensate cell destruction. These results confirm that experiments have to be performed in UP water in order to avoid an increase of cell number and an interference with treatment medium components. Moreover, the analysis of byproducts resulting from photocatalytic reaction on yeast cells will not interfere with the degradation of any external components. Consequently, all further experiments were conducted in ultra-pure (UP) water.

### 3.2. Influence of the photocatalytic reaction parameters on yeast cultivability

#### 3.2.1. Semiconductor concentration

Effect of $TiO_2$ concentration on cell cultivability was analyzed (Fig. 3a). Photocatalysis experiments were conducted using 0.05 to 1 g/l $TiO_2$ during a 5-h time course. Yeast cultivability was dependent of the semiconductor concentration, but no linear relationship between $TiO_2$ concentration and loss of cultivability was observed. Highest and lowest concentrations (1, 0.5 and 0.05 g/l) proved less efficient than average concentrations (0.25 and 0.1 g/l). Several parameters that are likely to interfere could explain these results. At low concentration of $TiO_2$ particles (0.05 g/l), all photons are not absorbed. On the contrary, an excess of particles could hide cells and block radiations. High $TiO_2$ concentrations have been previously related to a decrease of efficiency due to photoactivity saturation. Increasing $TiO_2$ concentration increases reactive surface sites but also prevents total light penetration through the treated suspension [10,38]. Moreover, as suggested by Carre et al. [39], in the case of *E. coli* cells, aggregation capacity of $TiO_2$ particles with yeast cells might increase with $TiO_2$ concentration. Their mode of aggregation by itself may also be concentration-dependent and influence the reaction. According to our experimental conditions, 0.1 g/l was found to be optimal to inactivate yeast cells. It is not surprising that this value did not correspond to the optimal concentration (0.25 g/l) determined for *E. coli* bacterial cells [40]. Indeed, yeast and bacterial cells do not have the same sizes (yeast cells are almost five times bigger) and are coated by chemically distinct cell wall. These

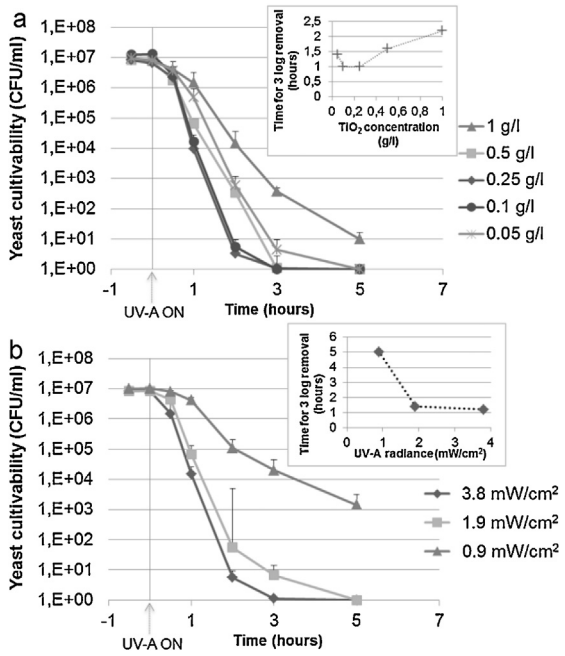


**Fig. 3.** Monitoring yeast cultivability on YPG medium. (a) Effects of different $TiO_2$ concentrations (0.05 g/l, 0.1 g/l, 0.25 g/l, 0.5 g/l and 1 g/l) under 3.8 mW/cm$^2$ UV-A radiance. (b) Effects of different UV-A intensities (3.8, 1.9 and 0.9 mW/cm$^2$) with 0.1 g/l $TiO_2$. Inserts represent the time necessary for 3 log removal as a function to $TiO_2$ concentrations (a) and UV-A intensities (b).

differences are likely to impact on the optimal concentration of nanoparticles.

### 3.2.2. UV-A radiance intensity

The effect of UV-A radiance intensity was investigated using the optimal $TiO_2$ concentration of 0.1 g/l. Monitoring yeast cell cultivability after exposure to different UV-A radiance intensity (3.8, 1.9 and 0.9 mW/cm$^2$) showed that lower intensity led to lower inactivation efficiencies (Fig. 3b). After 5 h of treatment using 0.9 mW/cm$^2$, 1000 cells remained cultivable, while no cultivable cells were detected when higher intensities were used. Close inactivation profiles were obtained with 1.9 and 3.8 mW/cm$^2$ intensities, suggesting that, at these values, reaction rate became independent of radiant flux [38]. Indeed, a higher energy means a higher activation of the semiconductor generating more $e^-/h^+$ reactive pairs but also an increasing number of limiting recombination events.

## 3.3. Impact of photocatalysis on yeast cell survival

### 3.3.1. Highlighting cell viability by double fluorescent dye staining

In order to study cell viability, we analyzed simultaneously i) the permeability of the plasma membrane using propidium iodide (PI) and ii) intracellular metabolic activity by using carboxyfluorescein diacetate (CFDA-AM). PI is an impermeable fluorescent DNA intercalating dye excluded from viable cells, assessing membrane integrity [41]. Membrane integrity is a parameter widely used to test cell viability [42]. However, because cell possesses membrane reparation mechanisms [43] and because membrane can be damaged (PI labeled cells) without cell death [44], another viability parameter to test the cell physiological state, was added. CFDA-AM is a non-fluorescent dye that, once cleaved in living cells by nonspecific intracellular enzymes (esterases), becomes fluorescent in green [45].

The efficiency of the PI/CFDA double staining in the presence of $TiO_2$ was validated by microscopic observations of stained cells exposed to non-activated $TiO_2$ suspension, to UVA photochemistry and to photocatalytic treatment (Fig. 4). For that purpose, the behavior of representative cell samples (several hundred of cells recovered from three different samplings) was checked. The presence of $TiO_2$ particles did not compromised the performances of the fluorochromes. Observations revealed that, after 1 h of exposure to $TiO_2$ suspended particles, yeast membrane permeability (0.5% PI labeled counted cells) was only slightly affected. Cells exposed to UV-A solely, were also affected (4% PI labeled counted cells). Moreover, microscopic observations conducted with $TiO_2$, with or without UV-A activation, revealed aggregates of cells embedded in nanoparticles. Size of the aggregates was heterogeneous and measured up to 100 μm. During photocatalysis, CFDA and PI double staining confirmed that cells were initially metabolically active (green) and had an intact membrane. After 15 min, red labeling (damaged membrane) was detected for cells showing simultaneously a green fluorescence due to an active metabolic activity (yellow-stained in merged images). After 30 min of treatment, most cells were labeled with both CFDA and PI, showing that yeast cells lost their membrane integrity (entry of PI and red labeling) but not their metabolic activity. After 1 h of treatment which corresponds to 0.13% of cultivable cells, most cells lost both membrane integrity and metabolic activity. These results suggest that despite the presence of a thick polysaccharidic cell-wall (Fig. 1), plasma membrane remain a favorite target for photocatalysis in yeast cells. Moreover, after 1 h of treatment yeast cells shape was preserved and regular suggesting that cell death is not directly related to a full disruption of the cellular envelopes that maintain yeast structure.

### 3.3.2. Monitoring cell death by flow cytometry

Cytometry allows to analyze a great number of cells, therefore providing statistical data to previous microscopic observation. Flow cytometry assays, combined with fluorescent staining were then used to investigate yeast viability during photocatalytic treatment. An untreated cell suspension was first analyzed (Fig. 5a) showing a variability of size and granularity parameters which reflects cell budding in early exponential phase cells. $TiO_2$ particles were characterized by their smaller size and granularity (Fig. 5a). When cells suspended with nanoparticles were analyzed, the two populations were easily distinguishable using these two parameters. However, cell granularity enhanced considerably due to the formation of aggregates of irregular sizes, as revealed by microscopic observations (Fig. 4). Cells exposed to photocatalytic treatment were then analyzed. At $t = 0$, while cells have been incubated for 30 min in $TiO_2$ suspension in the dark, both PI and CFDA parameters indicated the presence of living cells (Q4 zone, 98%) (Fig. 5b). This result revealed that cells exposed to $TiO_2$ particles alone for 30 min were not damaged. After 15 min, displacement of the signal (Q2 and Q1 zones, 8% and 3% respectively) indicated that simultaneously, cell membranes were starting to get damaged (increase of PI labeling) and enzymatic activity to get lost (Q4 zone, 87%). After 30 min, most cells (68.5%) presented both a damaged membrane and a loss of the metabolic activity (Q1) but 4.5% still have their enzymatic activity and membrane integrity (Q4). Double stained cells, observed by microscopy (in yellow) after 30 min of treatment (Fig. 4), represented about 25%. After one hour, this transient population of cells disappeared and all yeasts could be considered as dead (Q1 zone). Displacement of spots from Q2 to Q1 was progressive (Fig. 5b), which suggests that esterase enzymatic activity, supported by several distinct groups of intracellular proteins, decreased progressively. These results confirm the progressive inactivation of yeast suspension by loss of membrane integrity and loss of metabolic activity. Esterase inactivation can be due to potential photocatalytic oxidation or can be related to the loss of membrane integrity knowing that membrane perforation engender protein release and intracellular medium modifications disturbing enzyme activity.

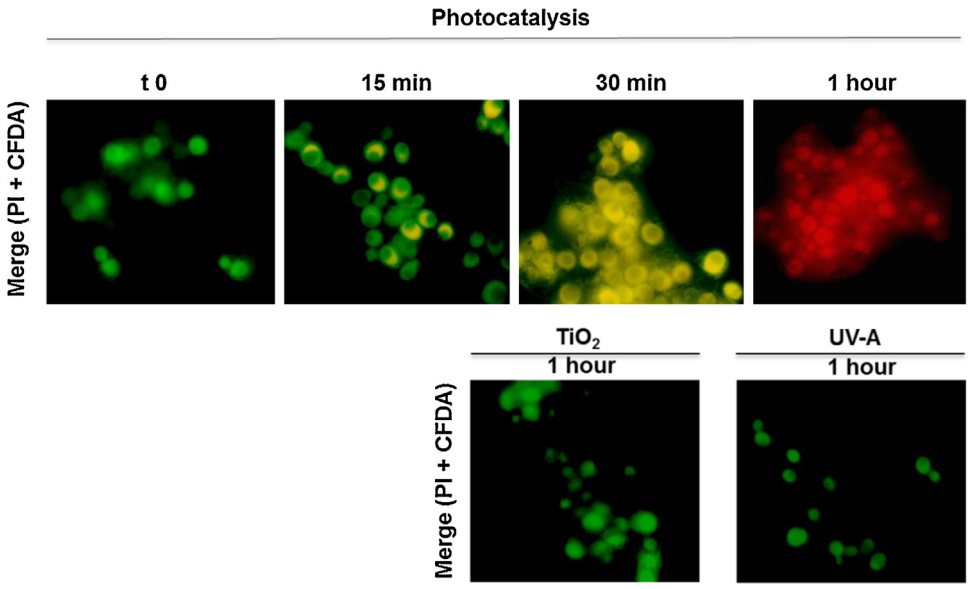


**Fig. 4.** Fluorescence microscopy of PI and CFDA double-stained cells after 1 h of photocatalytic treatment or 1 h of UV-A only, or of exposure to non-activated $TiO_2$ particles. Micrographs show representative samples of cells.

Damages to the membrane and loss of metabolic activity occurred rather simultaneously and evolved in parallel (Figs. 5b, 6a). However, a transient proportion of cells (detected from $t = 15$ min and no more detectable at $t = 1$ h) had a damaged membrane and were still metabolically active (Fig. 5b). This suggests that damages to the membrane do not imply an immediate enzyme activity break and cell death. Contrary to bacteria, respiration functions are not supported by plasma membrane in yeast and other eukaryotic organisms; but are compartmented to mitochondria (Fig. 1). These intracellular structures are bounded by a double

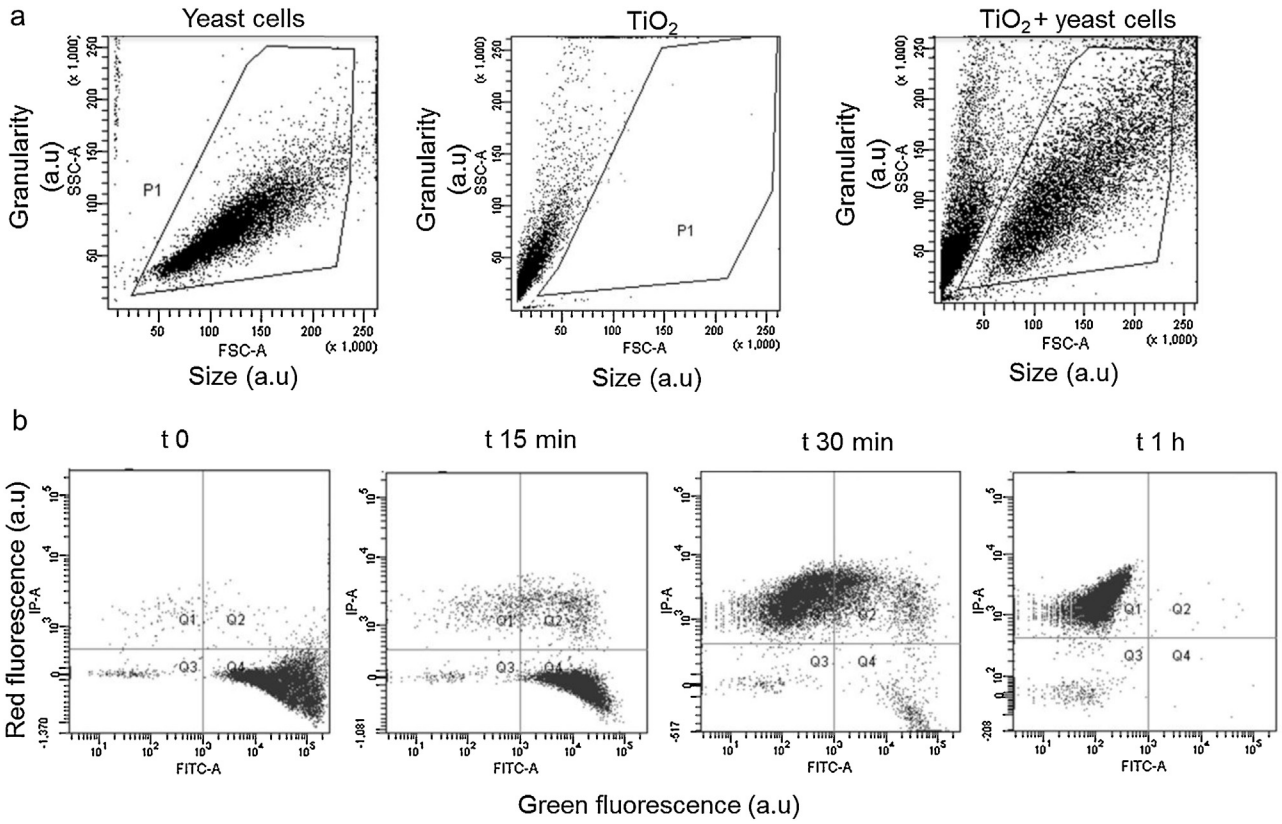


**Fig. 5.** Flow cytometry analyses. (a) Relative size (FSC-A axis) and granularity (SSC-A axis) of yeast cell suspension, $TiO_2$ suspension and yeast cells with $TiO_2$ particles (0.1 g/l) after 1 h without UV-A exposure. Yeast cells and $TiO_2$ particles were identified and delimited on the scatterplot, (b) red (PI) and green (CFDA-AM) fluorescence analysis of cells exposed to photocatalysis (0.1 g/l $TiO_2$ and 3.8 mW/cm$^2$ UV-A) for 0, 15 min, 30 min and 1 h. Red fluorescence (IP-A axis) and green fluorescence (FITC-A axis) spread in four zones: Q1 (red fluorescence only), Q2 (both red and green fluorescence), Q3 (no fluorescence) and Q4 (green fluorescence only) (For interpretation of the references to colour in this figure legend, the reader is referred to the web version of this article).

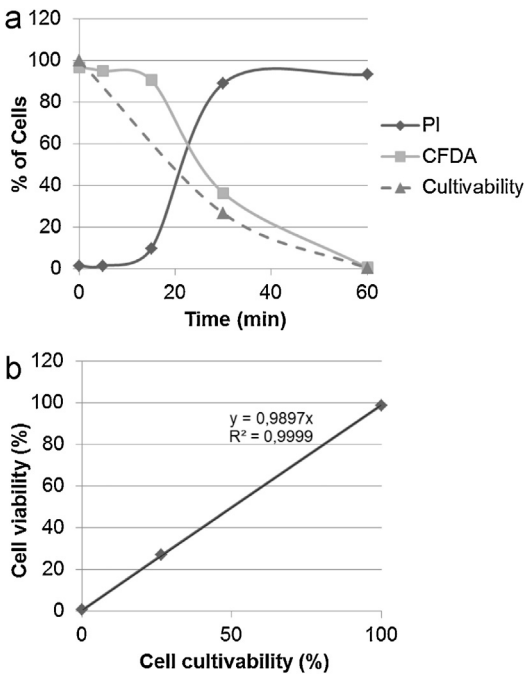


**Fig. 6.** Evolution of cell viability during photocatalysis. (a) Evolution of %PI, %CFDA labeled cells and of cultivability during treatment time (b) Correlation between cell viability and cell cultivability. Viable cell counts include metabolically active cells with or without damaged membranes (yellow + green cells) (For interpretation of the references to colour in this figure legend, the reader is referred to the web version of this article).

membrane composed of lipids and proteins. It would be interesting to know whether intracellular structures are targeted along with plasma membrane.

Cell viability comparison between cytometry and agar plate counts was performed (Fig. 6b). Our data revealed an excellent correlation between cell viability and cultivability only when double stained cells are considered as cultivable. This implies that cells with damaged membrane but still enzymatically active were still cultivable. Consequently, initial membrane damages are probably not sufficient to provoke death of metabolically active cells. Thus, considering exclusively the membrane status to characterize photocatalysis effects on cell viability appears to be insufficient.

Cultivability and viability investigations revealed that most cells (99%) were dead after 1 h of treatment and that no more cultivable cells could be detected after 5 h, (Fig. 2, 5). Further experiments were then performed to assess this total inactivation. In order to detect any growth arising from cells considered as inactivated, all cells ($2 \times 10^8$) used during a usual experiment and treated during 5, 7 and 20 h were harvest and used to inoculate fresh YPD growth liquid medium. After 5 days of incubation, cultivable cells were detected for cell suspensions treated 5 and 7 h, but not for 20 h of exposure. This suggests that over 5 h of photocatalysis, persistent cells, able of regrowth in optimal conditions, were detected neither by cultivability, nor by cytometry. Indeed, flow cytometry showed that 99% of the cells had a permeable plasma membrane and could be considered as dead cells after 1 h. Cultivability assay did not detect living cells after 5 h of exposure. Finally, this persistence test revealed that 20 h of treatment are necessary to guarantee no regrowth. This reveals that cultivability and viability analyzes methods are not sensitive enough to confirm a total photocatalytic inactivation.

### 3.4. Impact of photocatalysis on the environment: fate of yeast cells and release of byproducts

#### 3.4.1. Visualization of cells exposed to photocatalytic treatment

As we intended to investigate the release of byproducts in the environment during yeast cell exposure to photocatalytic treatment, we first checked if yeast cells were rapidly destructed upon treatment. For that purpose, treated cells were stained with Calcofluor white dye. Calcofluor white is a fluorescent dye that binds specifically to β1-3, β1-4-glucans and chitin cell wall

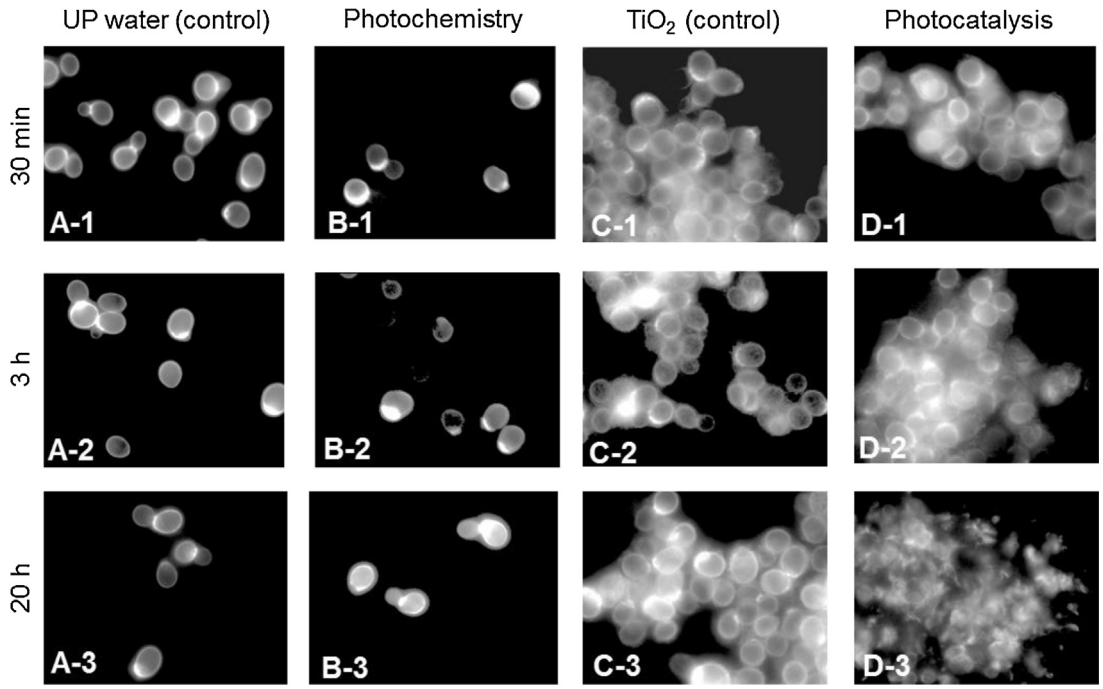


**Fig. 7.** Fluorescence microscopy of *S. cerevisiae*, stained with Calcofluor white dye. (A) without treatment, (B) after UV-A exposure (3.8 mW/cm$^2$), (C) after $TiO_2$ treatment (0.1 g/l) in the dark, (D) after photocatalytic treatment with 0.1 g/l $TiO_2$ and 3.8 mW/cm$^2$ UV-A irradiation. (1), (2) and (3) correspond to 30 min, 3 h and 20 h of treatment, respectively.

polysaccharides (Fig. 1). Binding to the cell wall occurs through hydrogen bonds which change the conformation of the molecule, leading to fluorescence. By detecting the fluorescence of the cell wall, it was then possible to visualize cell morphology during treatment, while cells were embedded with $TiO_2$ particles and got stuck in aggregates. Control experiments revealed that long time exposure (up to 20 h) to UP water or $TiO_2$ (Fig. 7), did not impact on cell shape. After 20 h of exposition to UV-A, yeast cells were dead (stained by PI) and presented a normal shape stained by Calcofluor dye (Fig. 7). On the contrary, cells exposed for 20 h to photocatalytic treatment revealed an irregular staining. At this stage, yeast cell wall was partially stained by Calcofluor white which could be explained by a potential disorganization of cell wall structure disturbing the dye binding. This reveals that once killed by photocatalysis cells are submitted to a continuous degradation process, destructuring the very thick and robust yeast cell wall [46]. Cell wall staining of yeast cells exposed to photocatalysis raises the question of nanoparticles infiltration mechanisms. It is usually assumed that oxidation takes place through surface-bound radicals which are not free to diffuse in the cell [8,11]. A direct contact between nanoparticles and cells has been proposed [15,21]. Porosity of the yeast cell wall is to limit the size and type of substances that may come in contact with the plasma membrane. The porosity of this structure has been estimated to an average of 36 Å [47] which could not allow the move of $TiO_2$ nanoparticles across the fibrillary network. However, penetration of nanoparticles through the wall, at early stages of exposure, may be facilitated by localized damaged areas that could facilitate the progression through a weakened structure and promote a direct contact to the membrane.

### 3.4.2. Monitoring of chemical byproducts

*3.4.2.1. Cations and anions.* Exposure to photocatalytic treatment led to membrane perforations (Figs. 4 and 5) and to the release of byproducts (Figs. 8–10). Ions released during photocatalytic process were monitored over a period of 20 h (Fig. 8). $K^+$ ions were rapidly released from the beginning of irradiation (Fig. 8a) in agreement with membrane damages observed by flow cytometry (Fig. 8c). $K^+$ ions were detected in larger amounts than $Na^+$. This is due to the fact that $K^+$ is the major cation inside yeast cells [48]. Beyond 5 h of treatment, a constant level for $K^+$ and $Na^+$ was detected. On the contrary, $NH_4^+$ was gradually released and its concentration increased during the time course of the reaction, suggesting that $NH_4^+$ was generated through the photocatalytic process, probably by being a byproduct of protein via amino acid degradation [49,50]. $NH_4^+$ could also be produced via the degradation of phosphatidylcholine and phosphatidylethanolamine, main yeast membrane phospholipids, or from derivative sugars like N-acetylglucosamine, monomer of chitin polymer component of the yeast cell wall [25].

Anions were gradually released in the reaction medium but in lower amounts than cations (Fig. 8b). After 20 h, $SO_4^-$ anions reached 30 μM, while $NH_4^+$ cations were detected over 150 μM. After 3 h of treatment the level of $SO_4^-$ exceeded the values of $Cl^-$ and $NO_3^-$ and gradually increased. Sulfate anions could originate from disulfide bounds or from protein containing sulfur atoms released through protein degradation. $NO_3^-$ was detected from the beginning of the reaction indicating that it could not be produced via the chemical transformation of $NH_4^+$ or protein containing amine groups, Ammonium is only degraded by photocatalysis at basic pH and amine groups are mainly transformed into ammonium [51]. Nitrite was not detected in treated suspension until 20 h. This could be due to its rapid degradation into $NO_3^-$ [52].

*3.4.2.2. Amino acids.* $NH_4^+$ cations released during photocatalysis could result from amino acids and protein degradation. In yeasts, proteins are abundantly present and exposed in cell wall (Fig. 1).

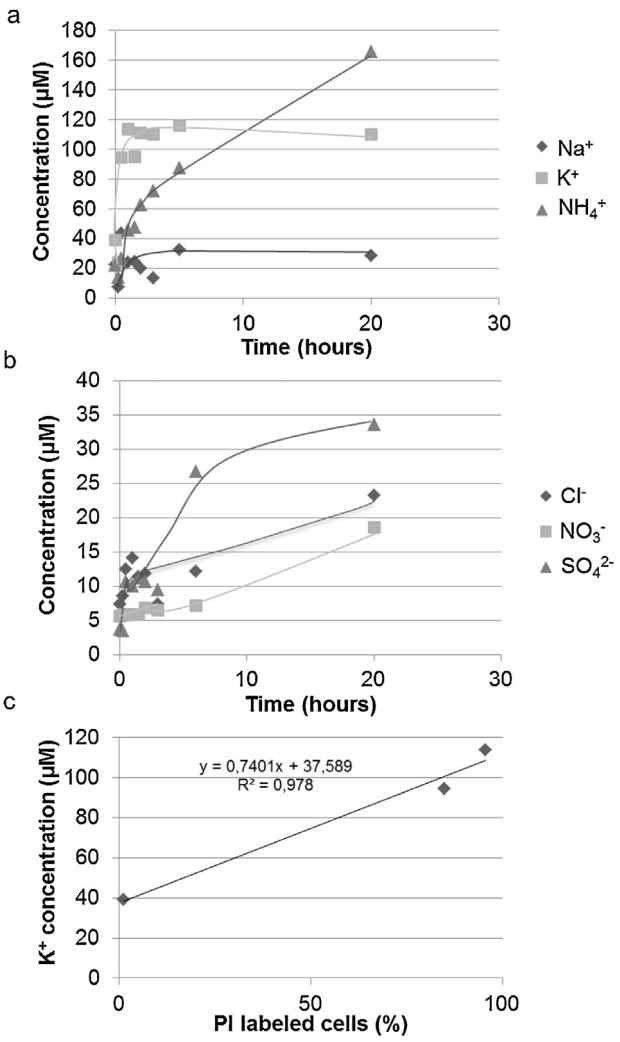


**Fig. 8.** Ion release from yeast cells during photocatalytic treatment. Evolution of cation (a) and anion (b) concentration released in UP water during photocatalytic inactivation of *S. cerevisiae* cells in the presence of 0.1 g/l $TiO_2$ and 3.8 mW/cm² UV-A. (c) Correlation curve between $K^+$ concentration and the percentage of damaged membrane cells (PI stained).

Thus, structural and transport proteins are part of membrane structure (cell and organelle membranes) and enzymatic proteins support cell activity in membranes and inside the cell. Loss of viability by enzymatic inhibition, membrane damages, and the protein rich cell wall exposed to photocatalysis suggested that proteins were targeted and consequently could release amino acids which are their base units. Amino acids were detected in the reaction medium during a 20 h time course photocatalytic experiment. Five major amino acids were identified: glutamic acid, aspartic acid, serine, glycine and alanine (Fig. 9). Glutamic acid appeared first and increased very rapidly (200 μM at 2 h) then decreased to disappear after 20 h. Aspartic acid revealed a similar profile but increased more slowly (1.5 times). A main peak corresponding to glycine and increasing over time was also detected from the beginning of the exposure. However, glycine amounts remained relatively constant (about 150 μM) over the 20 h of treatment. Serine and alanine were detected to a lower extent, during the treatment. As shown for aspartic and glutamic acids, serine and alanine levels decreased at 20 h. Those amino acids could be produced directly from photocatalytic degradation of proteins but could also arise from the degradation of other amino acids [49,50]. Based on the mechanisms of photocatalytic oxidation [49,50,53],

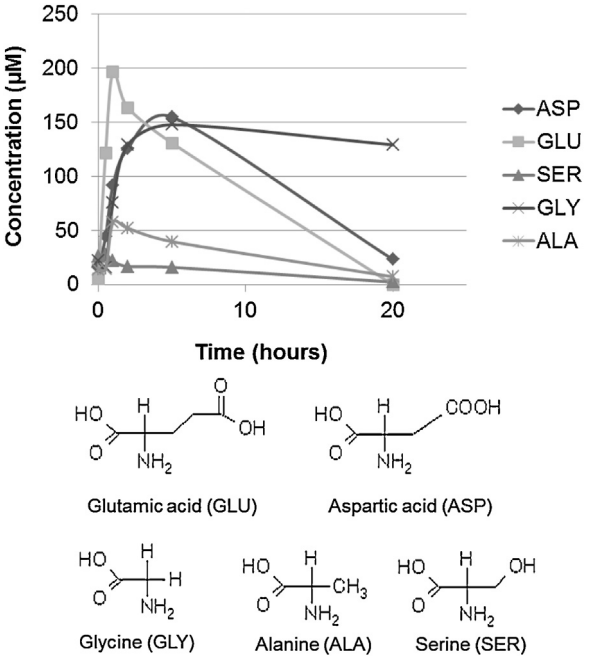


**Fig. 9.** Evolution of amino acids during photocatalysis of *S. cerevisiae* cells in the presence of 0.1 g/l of $TiO_2$ and 3.8 mW/cm$^2$ UV-A. Amino acids' chemical formulas are illustrated below the graph.

glutamic acid could be degraded into aspartic acid which in turn could be degraded into serine by successive oxidations and decarboxylations. Aspartic acid could also be degraded into alanine by reduction. Glycine level remained high over time, while the level of other amino acids decreased. This strongly suggests that photocatalysis degrades continuously amino acid byproducts and that glycine was probably produced via the chemical conversion of all amino acids [49,50].

*3.4.2.3. Carboxylic acids.* Oxalic and oxamic acids were the main carboxylic acids detected during yeast inactivation by photocatalysis (Fig. 10). Oxalic acid was detected from the beginning of the treatment and increased drastically over time, whereas oxamic acid was detected in relatively low amounts, beyond five hours of treatment. Oxamic acid could arise from photocatalytic damages to amino acids released during the degradation (Fig. 9) [49,50]. Oxalic acid may result from lipid peroxidation. Yeast plasma membrane is constituted from a phospholipid bilayer that could be drastically affected during loss of membrane integrity and cell stress generated by photocatalysis (Figs. 4 and 5). However, further analyses must be undertaken to determine the origin of these byproducts.

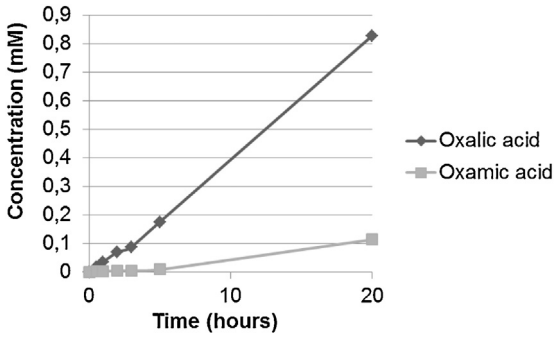


**Fig. 10.** Oxalic and oxamic acids formation during photocatalysis of *S. cerevisiae* cells in the presence of 0.1 g/l of $TiO_2$ and 3.8 mW/cm$^2$ UV-A.

## 4. Conclusions

We have studied the impact of UV-A photocatalysis treatment on the yeast *S. cerevisiae*, a model of eukaryotic unicellular organisms and fungal environmental contaminants. As compared to UV-A or $TiO_2$ controls, photocatalysis induced a drastic and quick loss of yeast cells cultivability. By monitoring cell death using flow cytometry and a double staining strategy, we evaluated simultaneously membrane permeability and enzyme activity in a population of treated cells. Loss of cultivability was directly connected to damages to the plasma membrane and loss of enzymatic activity. We concluded that plasma membrane constituted a key target of the photocatalytic process, irreversibly damaged despite the presence of a thick polysaccharidic cell wall. This suggested that $TiO_2$ particles could infiltrate the fungal wall to get in direct contact with the plasma membrane However, damage to the membrane does not imply cell death. Cells carrying membrane damage with remaining metabolic activity are still cultivable. Inactivation of enzyme activity suggested that intracellular proteins were progressively targeted, which could constitute a main antimicrobial element. Release of byproducts was investigated through the detection of amino acids, cations and anions, and carboxylic acids. Amino acids were rapidly detected in the reaction medium probably due to the degradation of glucomannoproteins present in cell wall. Among them, glycine was the only one maintained over time. This confirmed an attack of the protein pool and suggested that glycine was produced via the conversion of other amino acids. Cations and anions were rapidly released from yeast treated cells in accordance with the increase of membrane permeability. Among them, $SO_4^{-}$, $Cl^{-}$, $NO_3^{-}$ and $NH_4^{+}$ amounts increased continuously over an extended period of exposure. This suggested that those compounds were not only released from permeable cells, but chemically produced during treatment.

## Acknowledgments

The authors gratefully acknowledge the financial support of CNRS through the doctoral position fellowship of Sana Thabet. We are grateful to the members of the Génétique Moléculaire des Levures group for helpful support and advices. Finally, we acknowledge the support of the University of Lyon, University Lyon 1 and the CNRS.

## References

[1] J. Gamage, Z. Zhang, International Journal of Photoenergy (2010).
[2] H. Foster, I. Ditta, S. Varghese, A. Steele, Applied Microbiology and Biotechnology 90 (2011) 1847–1868.
[3] P.C. Maness, S. Smolinski, D.M. Blake, Z. Huang, E.J. Wolfrum, W.A. Jacoby, Applied and Environmental Microbiology 65 (1999) 4094–4098.
[4] P.K.J. Robertson, J.M.C. Robertson, D.W. Bahnemann, Journal of Hazardous Materials 211–212 (2012) 161–171.
[5] S. Malato, P. Fernández-Ibáñez, M.I. Maldonado, J. Blanco, W. Gernjak, Catalysis Today 147 (2009) 1–59.
[6] T.H. Bui, C. Felix, S. Pigeot-Remy, J.-M. Herrmann, P. Lejeune, C. Guillard, Journal of Advanced Oxidation Technologies 11 (2008) 510–518.
[7] J.M. Herrmann, C. Guillard, P. Pichat, Catalysis Today 17 (1993) 7–20.
[8] A. Mills, S. Le Hunte, Journal of Photochemistry and Photobiology A: Chemistry 08 (1997) 1–35.
[9] J.C. Ireland, P. Klostermann, E.W. Rice, R.M. Clark, Applied and Environmental Microbiology 59 (1993) 1668–1670.
[10] M. Cho, H. Chung, W. Choi, J. Yoon, Water Research 38 (2004) 1069–1077, 11T.
[11] T. Matsunaga, R. Tomoda, T. Nakajima, H. Wake, FEMS Microbiology Letters 29 (1985) 211–214.
[12] D.M. Blake, P.-C. Maness, Z. Huang, E.J. Wolfrum, J. Huang, W.A. Jacoby, Separation and Purification Methods 28 (1999) 1–50.
[13] D.D. Sun, J.H. Tay, K.M. Tan, Water Research 37 (2003) 3452–3462.
[14] A.G. Rincón, C. Pulgarin, Applied Catalysis B: Environmental 49 (2004) 99–112.
[15] G. Gogniat, M. Thyssen, M. Denis, C. Pulgarin, S. Dukan, FEMS Microbiology Letters 258 (2006) 12–24.
[16] P. Liu, W. Duan, Q. Wang, X. Li, Colloids and Surfaces B 78 (2010) 171–176.

[17] A.K. Benabbou, C. Guillard, S. Pigeot-Rémy, C. Cantau, T. Pigot, P. Lejeune, Z. Derriche, S. Lacombe, Journal of Photochemistry and Photobiology A: Chemistry 219 (2011) 101–108.
[18] S. Pigeot-Rémy, F. Simonet, E. Errazuriz-Cerda, J.C. Lazzaroni, D. Atlan, C. Guillard, Applied Catalysis B: Environmental 104 (2011) 390–398.
[19] S. Pigeot-Rémy, F. Simonet, D. Atlan, J.C. Lazzaroni, C. Guillard, Water Research 46 (2012) 3208–3218.
[20] T. Matsunaga, R. Tomoda, T. Nakajima, N. Nakamura, T. Komine, Applied and Environmental Microbiology 54 (1988) 1330–1333.
[21] C. Guillard, T.H. Bui, C. Felix, V. Moules, B. Lina, P. Lejeune, Comptes Rendus Chimie 11 (2008) 107–113.
[22] T. Saito, T. Iwase, J. Horie, T. Morioka, Journal of Photochemistry and Photobiology, B 14 (1992) 369–379.
[23] J. Deacon (Ed.), Fungal Biology, fourth ed., Blackwell publishing, USA, 2005.
[24] D.H. Jennings, G. Lysek, Fungal Biology: understanding the fungal lifestyle, Bios (1999).
[25] G.M. Walker, Yeast Physiology and Biotechnology, John Wiley & Sons, Cichester, 1998.
[26] D. Botstein, G.R. Fink, Science 240 (1988) 1439–1443.
[27] A. Erkan, U. Bakir, G. Karakas, Journal of Photochemistry and Photobiology A: Chemistry 184 (2006) 313–321.
[28] K.P. Kühn, I.F. Chaberny, K. Massholder, M. Stickler, V.W. Benz, H.G. Sonntag, L. Erdinger, Chemosphere 53 (2003) 71–77.
[29] C. Maneerat, Y. Hayata, International Journal of Food Microbiology 107 (2006) 99–103.
[30] C. Sichel, J. Tello, M. de Cara, P. Fernández-Ibáñez, Catalysis Today 129 (2007) 152–160.
[31] C. Sichel, M. de Cara, J. Tello, J. Blanco, P. Fernández-Ibáñez, Applied Catalysis B: Environmental 74 (2007) 152–160.
[32] S. Hohmann, Microbiology and Molecular Biology Reviews 66 (2002) 300–372.
[33] K. Kasemets, A. Ivask, H.-C. Dubourguier, A. Kahru, Toxicology in Vitro 23 (2009) 1116–1122.
[34] S. Kozmin, G. Slezak, A. Reynaud-Angelin, C. Elie, Y. de Rycke, S. Boiteux, E. Sage, Proceedings of the National Academy of Science 02 (2005) 13538–13543.
[35] J. Cadet, E. Sage, T. Douki, Mutation Research 571 (2005) 3–17.
[36] A. Moncayo-Lasso, L.E. Mora-Arismendi, J.A. Rengifo-Herrera, J. Sanabria, N. Benitez, C. Pulgarin, Photochemistry & Photobiological Sciences 11 (2012) 821–827.
[37] A.-G. Rincón, C. Pulgarin, Applied Catalysis B: Environmental 51 (2004) 283–302.
[38] J.M. Herrmann, Catalysis Today 53 (1999) 115–129.
[39] G. Carre, D. Benhamida, J. Peluso, C.D. Muller, M.-C. Lett, J.-P. Gies, V. Keller, N. Keller, P. Andre, Photochemistry & Photobiological Sciences (2012), DOI: 10.1039/c2pp25189b.
[40] A.K. Benabbou, Z. Derriche, C. Felix, P. Lejeune, C. Guillard, Applied Catalysis B: Environmental 76 (2007) 257–263.
[41] D. Deere, J. Shen, G. Vesey, P. Bell, P. Bissinger, D. Veal, Yeast 14 (1998) 147–160.
[42] B.P. Tracy, S.M. Gaida, E.T. Papoutsakis, Current Opinion in Biotechnology 21 (2010) 85–99.
[43] R.A. Steinhardt, Annals of the New York Academy of Sciences 1066 (2006) 152–165.
[44] H.M. Davey, P. Hexley, Environmental Microbiology 13 (2011) 163–171.
[45] L. Chan, A. Wilkinson, B. Paradis, N. Lai, Journal of Fluorescence 22 (2012) 1301–1311.
[46] F.M. Klis, A. Boorsma, P.W.J. De Groot, Yeast 23 (2006) 185–202.
[47] P. Gerhardt, J.A. Judge, Journal of Bacteriology 87 (1964) 945–951.
[48] A. Rodrïguez-Navarro, BBA 1469 (2000) 1–30.
[49] L. Elsellami, F. Vocanson, F. Dappozze, E. Puzenat, O. Païsse, A. Houas, C. Guillard, Applied Catalysis A – General 380 (2010) 142–148.
[50] L. Elsellami, F. Vocanson, F. Dappozze, R. Baudot, G. Febvay, M. Rey, A. Houas, C. Guillard, Applied Catalysis B: Environmental 942010192-199.
[51] E.M. Bonsen, S. Schroeter, H. Jacobs, J.C. Broekaert, Chemosphere 35 (1997) 1431–1445.
[52] S. Chen, G. Cao, Desalination 194 (2006) 127–134.
[53] C. Guillard, Journal of Photochemistry and Photobiology A: Chemistry 135 (2000) 65–75.